The Journal of Experimental Biology 206, 4363-4377

doi:10.1242/jeb.00679

Three-dimensional hindlimb kinematics of water running in the plumed basilisk lizard (*Basiliscus plumifrons*)

S. Tonia Hsieh

Department of Organismic and Evolutionary Biology, Harvard University, Cambridge, MA 02138, USA

(e-mail: sthsieh@oeb.harvard.edu)

Accepted 18 August 2003

Summary

Much of what is known about tetrapod locomotion is based upon movement over solid surfaces. Yet in the wild, animals are forced to move over substrates with widely varying properties. Basilisk lizards are unique in their ability to run across water from the time they hatch to adulthood. Previous studies have developed mechanical models or presented theoretical analyses of running across water, but no detailed kinematic descriptions of limb motion are currently available. The present study reports the first three-dimensional kinematic descriptions of plumed basilisk lizards (*Basiliscus plumifrons*) running across water, from hatchling (2.8 g) to adult (78 g) size range. Basilisks ran on a 4.6 m-long water track and were filmed with two synchronized high-speed cameras at 250 frames s^{-1} and 1/1250 s shutter speed. All coordinates were transformed into three dimensions using direct linear transformation. Seventy-six kinematic variables and six morphological variables were measured or calculated to describe the motion of the hindlimb, but only 32 variables most relevant to kinematic motion are presented here.

Kinematic variation among individuals was primarily related to size differences rather than sprint speed. Although basilisk lizards applied some of the same strategies to increase running velocity across water as other tetrapods do on land, their overall kinematics differ dramatically. The feet exhibit much greater medio-lateral excursions while running through water than do those of other lizards while running on land. Also, whereas the hindlimb kinematics of other lizards on land are typically symmetrical (i.e. limb excursions anterior to the hip are of similar magnitude to the limb excursions aft of the hip), basilisks running through water exhibit much greater excursions aft than they do anterior to the hip. Finally, ankle and knee flexion in early stance is a defining feature of a tetrapod step during terrestrial locomotion; yet this characteristic is missing in aquatic basilisk running. This may indicate that the basilisk limb acts primarily as a force producer – as opposed to a spring element – when locomoting on a highly damping surface such as water.

Key words: water running, hindlimb kinematics, bipedal locomotion, ontogeny, scaling, plumed basilisk lizard, Iguanidae, *Basiliscus plumifrons.*

Introduction

Basilisk lizards (*Basiliscus* sp.) are characterized by their remarkable ability to run across water. Numerous observations have reported both juvenile and adult lizards jumping off branches or starting from shore and running bipedally across a body of water as a method of predator evasion (Barden, 1943; Laerm, 1973; Maturana, 1962; Rand and Marx, 1967). How basilisks accomplish this marvelous feat remains a mystery. Existing literature provides primarily qualitative descriptions (Barden, 1943; Laerm, 1973; Rand and Marx, 1967), with very little quantitative measurement of these lizards' movements. More quantitative data (Glasheen and McMahon, 1996a,b) are based upon theoretical or mechanical models of basilisk feet.

Lizard locomotion has served as a model system for morphological and functional studies because of the tremendous variation exhibited in life history and growth patterns (Irschick and Jayne, 1999). Although substantial descriptions of terrestrial quadrupedal kinematics in lizards now exist (Fieler and Jayne, 1998; Irschick and Jayne, 1998, 1999, 2000; Jayne and Irschick, 1999; Reilly and Delancey, 1997a,b), very little is known about bipedal locomotion in lizards (except Irschick and Jayne, 1999). Bipedality has evolved numerous times among lizards – most notably among those that live in sandy, rocky or open environments or lizards classified as having semi-aquatic or semi-arboreal lifestyles (Snyder, 1952). Substantial size variation also exists between juvenile and adult lizards – juveniles often increase in mass by as much as 50 times by adulthood (Irschick and Jayne, 2000). How such a size difference affects locomotor capability is an issue of general interest among physiologists and morphologists. Most of what is known about the effects of size on limbed locomotion was derived from comparisons between animals from wide-ranging phylogenetic taxa (e.g. Alexander, 1977; Alexander and Jayes, 1983; Bertram and Biewener, 1992; Biewener, 1983; Cavagna et al., 1977; Farley et al.,

1993; Heglund et al., 1974). Far fewer studies have examined ontogenetic effects on locomotion within one species (Garland, 1985; Huey and Hertz, 1982; Irschick and Jayne, 2000). Although these studies have given valuable insight into how the mechanics of motion change with size, they have all focused on movement over stiff surfaces. A damping surface such as water exaggerates the effects of size on motion because increased mass results in disproportionate increases in energetic requirements. Whereas locomotion on stiff surfaces permits energy storage in muscles and tendons, damping substrata dissipate this energy, thereby requiring more energy to be expended with the subsequent step (Lejeune et al., 1998).

Aquatic locomotor capability among basilisks is size dependent; juveniles more frequently run towards water to escape threats and appear to run through water more easily than do adults (Barden, 1943; Laerm, 1973; Rand and Marx, 1967). A hydrodynamic model developed by Glasheen and McMahon (1996a,b) showed that basilisks are most constrained by their size-dependent ability to produce forces on water. Large lizards can produce relatively much less of a slap impulse than do small lizards. Additionally, all lizards are potentially subject to hydrodynamic drag created by water surrounding their submerged foot. Glasheen and McMahon (1996a,b) reported that the basilisks – especially the large adults – extract their feet from an air cavity created during the stride, prior to cavity collapse. This mechanism allows large lizards to minimize hydrodynamic drag on the foot.

Even though the results from Glasheen and McMahon's studies give substantial insight regarding mechanisms of water running, there were no detailed descriptions of how basilisks move when running across water. The only previously existing detailed basilisk water-running kinematics documented several angular excursions of limbs (Laerm, 1973), sprint velocities (Rand and Marx, 1967) and some qualitative descriptions of motion (Barden, 1943; Laerm, 1973; Rand and Marx, 1967). Two of these three studies were based on observations in the field (Barden, 1943; Rand and Marx, 1967), and one was based on two-dimensional data (Laerm, 1973). Lizards are generally characterized as quadrupedal sprawlers (Russell and Bels, 2001). This limb posture forces lizards' limb movements to be highly complex through space. Kinematic measurements in three dimensions are therefore critical for accuracy.

The goals of the present study are: (1) to present the first detailed three-dimensional kinematic descriptions of basilisk water running; (2) to quantitatively examine the effects of size and sprint speed on water-running capability and (3) to compare these data from aquatic running with data on terrestrial lizard locomotion in the existing literature. I expected that large basilisks would sink deeper into the water as a result of their greater mass and therefore exhibit greater limb excursions along all three axes than would smaller basilisks. The concomitant increase in energetic requirements would thus limit larger basilisks to sprinting at a proportionately slower speed than do juvenile basilisks. As compared with terrestrial runs, basilisks should exhibit a more extended propulsive phase during aquatic running, so that more time during a stride would be dedicated to the generation of thrust and lift. Also, limb posture should be more crouched to enable greater force generation.

Materials and methods

Animals

Thirty plumed basilisk lizards [*Basiliscus plumifrons* (Cope 1876)] were obtained from a reptile wholesale supplier (Quality Reptiles, Los Angeles, CA, USA). Animals were housed in pairs in 113-liter aquaria and fed crickets and mealworms, dusted with vitamin and calcium supplement, and an occasional pinkie mouse. Full-spectrum fluorescent bulbs that were high in UVB, were set to a 12 h:12 h light:dark schedule, and ceramic heating elements were provided 24 h a day to allow the animals to thermoregulate at their preferred body temperature. Data presented here represent runs from animals ranging in mass from 2.8 g to 78 g.

To assess how basilisks' shape changes with growth, I measured each animal's mass, snout–vent length (*SVL*), femur length, tibia length and foot length (defined as the distance from the heel to the tip of the fourth toe). Leg length (*LL*) was defined as the sum total of femur, tibia and foot lengths. To determine the mass of the tail relative to the total mass of the basilisk, the tails of three preserved striped basilisk (*Basiliscus vittatus*) specimens – ranging in size from hatchling to adult – were removed, just caudad of the cloaca, and weighed. In addition, two plumed basilisks (a juvenile and an adult) were sacrificed and their tails similarly removed and weighed. The relative mass of the tail in plumed basilisks coincided with that in striped basilisks. Longitudinal location of the basilisk's center of mass was determined by tying a thread around the body of a preserved specimen and repositioning the thread until the body balanced horizontally.

Experimental protocol

A 4.6 m-long water track was built by gluing together two 379-liter glass aquaria that had the ends removed. A 0.2 m-long platform was glued to each end of the track, 0.4 m above the bottom of the tank, with a hide box and heating element placed at the left end (i.e. at the end of the run). Tanks were filled with water such that each platform was flush to the water surface. All runs by medium juvenile to adult animals extended the full length of the water track. The track was shortened to 1.5 m for smaller juveniles and hatchlings (mass <10 g). Axes were oriented such that the positive *x*-axis pointed in the direction of travel, the positive *y*-axis pointed up and the positive *z*-axis pointed to the left of the running lizards. A plastic wall marked with a 2 cm×2 cm grid was mounted parallel to the front of the tank such that it could be repositioned to narrow the width of the track. All runs presented here represent the basilisks' preferred aquatic sprint speed since it was not possible to control the speed at which the basilisks ran (see Statistics section for more detailed discussion). The digitized speeds for basilisks running across the water track in this study were

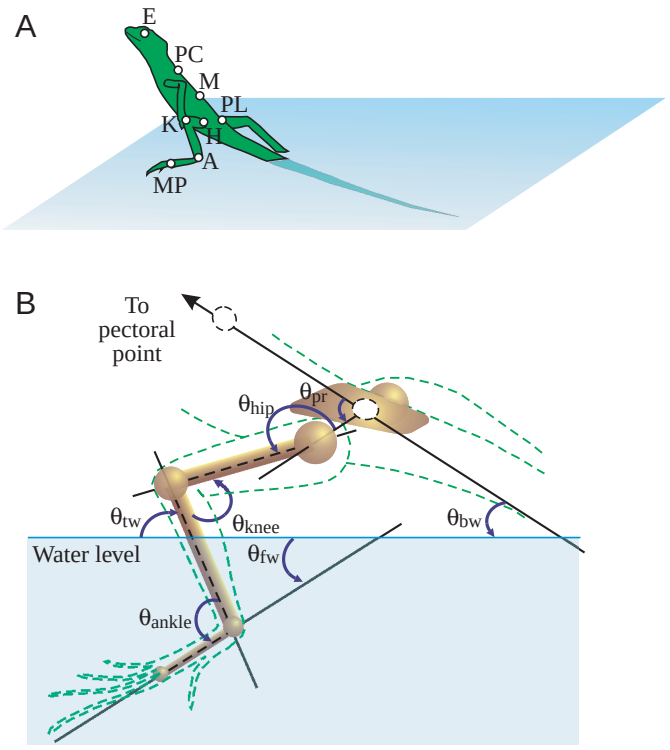

Fig. 1. Kinematic landmarks and calculated angles describing the motion of the hind limb. (A) Eight points marked with reflective paint. The abbreviations are as follows: E, eye, positioned between the eyes in the dorsal aspect; the center of the eye was digitized in the lateral aspect; PC, pectoral, positioned midway between the shoulder joints; M, a point midway between pectoral and pelvis points; PL, pelvis, midpoint between palpated positions of acetabula; H, hip acetabulum; K, knee; A, ankle; MP, foot, positioned over the metatarsal–phalangeal joint of the longest (fourth) digit. Even though all of these points were digitized, only data from the hind limb points are presented in this paper. (B) Three-dimensional angles are labeled as follows: θ_{hip}, hip angle formed by two planes containing lines PL–H and H–K; θ_{knee}, knee angle formed by two planes containing lines H–K and K–A; θ_{ankle}, ankle angle formed by two planes containing lines K–A and A–MP; θ_{fw}, angle formed between the foot (line MP–A) and the water surface; θ_{tw}, angle formed by the tibia (line K–A) to the water surface; θ_{bw}, angle formed between the torso (line PC–PL) and the water surface. Pelvic rotation was measured as a two-dimensional angle, θ_{pr}, formed by two planes containing lines H–PL and E–PL. All joint angles greater than 90° indicate joint extension, and all joint angles less than 90° indicate joint flexion. Negative values of θ_{fw} indicate a toe-up foot position, whereas positive values indicate a toe-down foot position. Angles were measured in the counterclockwise direction.

within the range of those speeds previously recorded in field conditions (Rand and Marx, 1967).

Each run was filmed with two synchronized, high-speed Redlake PCI500 cameras (Redlake Imaging, Morgan Hill, CA, USA) operating at 250 frames s^{-1} with a 1/1250 s shutter speed. Lizards took a minimum of three to four strides before entering the field of view, thus ensuring that basilisks were running at a constant speed. Each stride was represented by 26–42 frames in each camera. Cameras were oriented such that one camera filmed the lateral view, and the other the dorsal view. Basilisks were placed on the platform on the right side of the track and encouraged to run by squeezing the base of the tail and tapping their back. Prior to each trial, eight landmarks were painted on each basilisk to facilitate digitizing (Fig. 1A). Four points marked the midline: between the eyes on the dorsum of the head (E), midway between the shoulders on the pectoral girdle (PC), midway between the hips on the pelvic girdle (PL) and midway between PC and PL on the midline (M). Four points marked the left hindlimb: hip (H), knee (K), ankle (A) and at the fourth metatarsal–phalangeal joint, which will be referred to as the MP point or foot.

A run was deemed acceptable if the lizard ran truly bipedally such that its hands did not touch the water throughout the stride. Some leniency was granted for lizards weighing more than 60 g as they usually sank so far into the water that some contact of the hands with the water was inevitable. Among these heaviest animals, the run was accepted if the lizard's hands touched the water but it still kept its torso elevated above the water surface. For all lizards, regardless of size, runs were immediately discarded if the basilisk exhibited any clear breaks in motion (e.g. as a result of tripping), if any part of the limb or foot contacted any portion of the track's walls or if the lizard was running at a clear angle to the track (i.e. towards a wall). As a result of these selection criteria, out of the 30 animals filmed, only 11 of the runs from 11 animals were selected for data analysis – each of the selected runs represents the only run analyzed from an individual lizard. The drawback of having so few acceptable runs was that the data could not be analyzed for individual variation. However, as a result of using stringent selection criteria, the data presented in this paper represent exclusively true bipedal water runs, and each data point represents a statistically independent event.

Direct linear transformation

The challenge of photogrammetric camera calibrations resides in accurately relating two-dimensional camera images to actual three-dimensional space. This is often not trivial because cameras being oriented slightly off-axis or lens distortions – caused by short filming distances or inconsistencies in the lens (Hatze, 1988; Hedrick et al., 2002) – introduce errors into the final transformations. These errors are minimized in most three-dimensional kinematics studies by limiting all motion to the center of the field of view, such as on a treadmill or in a flow tank. As a result, it is possible to simply overlay the *x*–*y* and *x*–*z* coordinates from lateral and dorsal views to obtain the three-dimensional coordinates. This study required fixed camera locations with the basilisks passing through the field of view; as a result, lens distortions at the edges of the field were problematic. To correct for distortions, all digitized points were transformed into three dimensions using a direct linear transformation (DLT) algorithm implemented in MATLAB (The MathWorks, Inc., Natick, MA, USA) by Christoph Reinschmidt and Ton van den Bogert of the University of Calgary (1997).

DLT is a technique in which 11 coefficients are calculated

to correct for linear forms of image distortion (Woltring and Huiskes, 1990). These coefficients determine the positions of the cameras relative to each other and a pre-set coordinate system. Once the camera positions are known, a point seen in at least two cameras can then be reconstructed in three-dimensional space. A minimum of 15 non-coplanar points that maximally fill the area of interest is needed for this technique to work properly (Reinschmidt and Bogert, 1997). The calibration object was built from Duplo Lego (Switzerland). Eighteen non-coplanar points were available on the calibration object (0.27 m×0.10 m×0.15 m; length × width × height), with a minimum of 16 non-coplanar points visible in both cameras. For basilisks weighing up to 10 g, the calibration object filled the entire volume of the recording space. Although the field of view was greater when filming larger basilisks, the maximum field of interest measured 0.34 m×0.11 m×0.18 m (length × width × height); so the calibration object always filled at least 80% of the recording space.

Kinematic variables

For ease of analysis, I divided each stride into four phases based on the primary direction of motion of the MP joint (Fig. 2), similar to those defined by Glasheen and McMahon (1996a,b). The slap phase began when MP first contacted the water, moving primarily downwards (negative *y*-direction). The stroke phase began when MP moved in the negative *x*-direction (opposite to the running direction). Recovery up was defined as when MP began moving upwards such that part of this phase is completed under water and part of this phase is completed through the air. Recovery down completed the stride cycle, beginning when MP started moving down and ending at the start of the next slap phase. As compared with terrestrial locomotion, the slap and stroke phases appear to be functionally equivalent to the stance period, whereas the recovery up and recovery down phases appear to be equivalent to the swing period.

As a result of the extremely complex limb movement during water running, a large number of variables were necessary to clearly describe limb positions and motion. All kinematic variables, unless otherwise specified, were measured in three dimensions. Angular data were calculated with a custom MATLAB program and analyzed in Microsoft Excel. Digitizing error was calculated to be between ±0.2 mm for points that were never submerged through the stride and

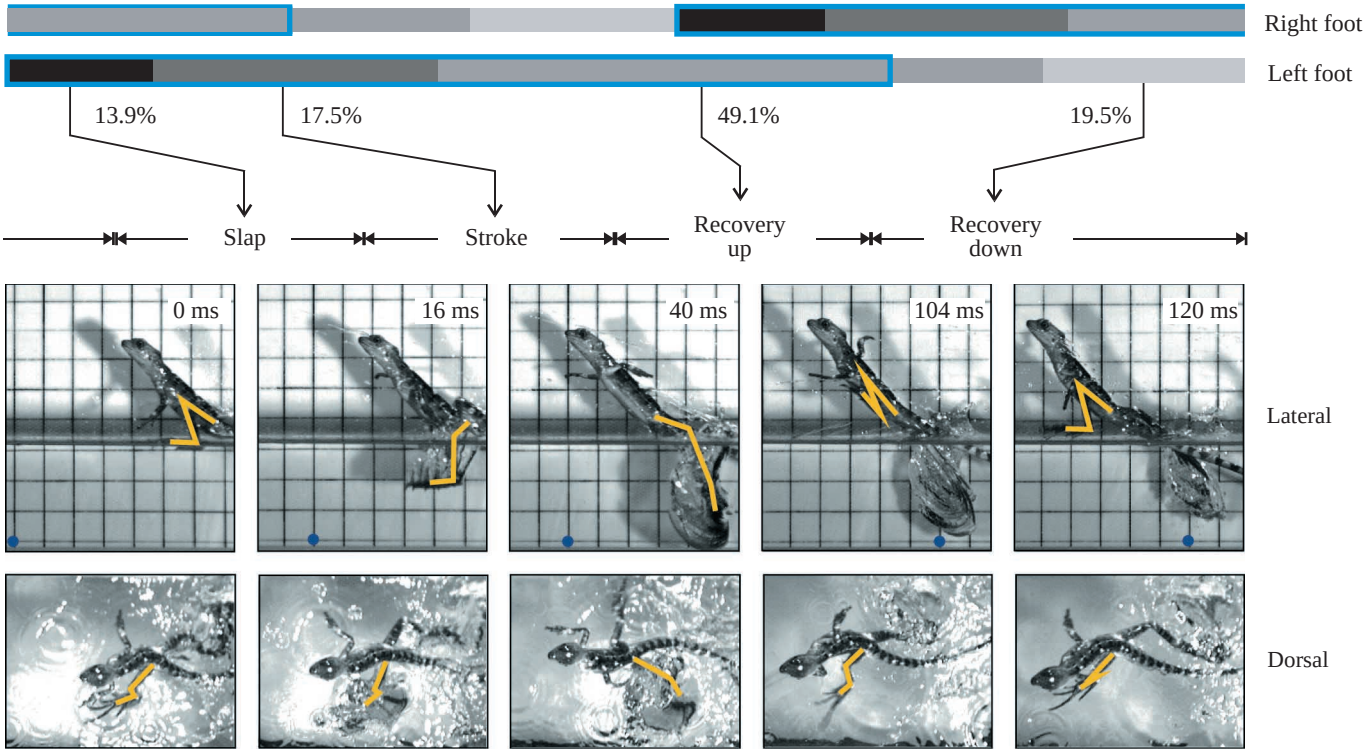

Fig. 2. Simultaneous lateral and dorsal images from high-speed video, illustrating the four phases of a stride. Some kinematic landmarks are visible in the dorsal view. Time for each frame of this run (20.8 g lizard, 1.4 m s^{-1}) is shown in milliseconds in the upper right corner of each lateral view frame. The left foot is highlighted in both the lateral and dorsal images to show foot position at each phase. The blue circle in each lateral frame marks the same grid intersection to serve as a global point of reference that does not move with the lizard. Bars at the top of the figure represent footfall patterns for the right and left feet for this run. Colors of each section indicate stride phase, progressing from black to light gray: slap, stroke, recovery up and recovery down. See text for details on phase determination. The light blue box around the bars indicates when the foot is in the water. Numbers below the left foot footfall pattern indicate mean percent duration of each phase for all analyzed runs, simplified for clarity. Actual values (mean ± S.E.M.) from slap to recovery down averaged for 11 basilisk lizards are: 13.9±5.2%, 17.5±5.1%, 49.1±4.4% and 19.5±6.8%.

±0.5 mm for points that were submerged in water, and therefore more difficult to digitize. For each trial, I calculated a series of variables describing the linear and timing characteristics of a stride, based upon previous studies of terrestrial kinematics (Fieler and Jayne, 1998; Gatesy and Biewener, 1991; Irschick and Jayne, 1999, 2000; Jayne and Irschick, 1999). These included whole-limb movements, movements of the hindlimb joints, and limb postures.

To characterize the stride, general variables describing whole-limb movements included mean forward velocity ($\mathbf{U}_{avg}$), stride length, stride duration and frequency, and duty factor (*Df*). $\mathbf{U}_{avg}$ was calculated by averaging the derivative of positional coordinates. Stride length was the three-dimensional distance traversed by the MP joint between footfalls by the left foot, and stride duration was the time to move one stride length. Stride frequency was defined as the inverse of stride duration. Duty factor for terrestrial locomotion is the ratio of stance duration to total stride duration. The stance phase in terrestrial locomotion is primarily responsible for production of thrust, and the swing phase brings the foot forward to begin the next step. In the case of lizards running through water, this distinction was not so clear since part of recovery up takes place while the foot is still submerged and moving slightly backwards. As a result, I calculated duty factor in two ways: the fraction of a stride in which the foot is submerged in water (Df_{sub}) and the fraction of a stride dominated by the slap and stroke phases (Df_{stance}).

To describe the movements of the hindlimb joints, coordinates of each joint in space and relative to the hip were digitized, and their velocities calculated. By holding the hip stationary, it was possible to isolate the limb movements from pelvic roll and thus facilitate visualization of how the limb points moved relative to each other through one stride cycle (Fieler and Jayne, 1998). Motions of the right limb are assumed to be mirror motions of the left limb during the subsequent step. Velocities of each of the hind limb points were calculated by taking the derivative of each joint's positional data along each of the three axes. Magnitude reflects the speed, and sign reflects the direction of movement (see above for axis assignments). The maximum and minimum values in each direction for each of the three limb joints (hip, knee and ankle) were used to calculate joint excursions (ΔX, ΔY and ΔZ). For example, the total horizontal excursion of the knee joint in one stride (ΔX_{knee}) was calculated as $X_{knee,max} - X_{knee,min}$.

Limb posture during a stride was described primarily by two linear variables. Effective limb length (*eLL*) was a linear quantification of whole-limb flexion or extension. Measured as the three-dimensional distance between the hip and the MP points, a smaller value reflects a more crouched limb posture while a greater value indicates a more extended limb posture. Effective limb length was quantified at footfall (eLL_{ff}), and the mean was determined for the stroke phase (eLL_{stroke}).

Joint positions were described by four linear and 15 angular variables, as described below. Hip position was quantified with two variables: mean height to the water surface (Y_{hip}) and total vertical excursion (ΔY_{hip}), calculated as the difference between the maximum and minimum heights of the hip in a stride ($Y_{hip,max}$–$Y_{hip,min}$). $Y_{hip,min}$ reflected how far the animal sank into the water. The remaining variables are all angular measurements. Fig. 1B provides a graphical explanation of how angles were measured. Three-dimensional joint angles (θ_{hip}, θ_{knee} and θ_{ankle}) were calculated from positional data at footfall (e.g. $\theta_{hip,ff}$) and at the end of stance (e.g. $\theta_{hip,es}$). Minimum joint angle at stance (e.g. $\theta_{hip,min}$) was also calculated. Joint flexion resulted in decreasing angles, and joint extension resulted in increasing angles. The amount of extension and flexion of each joint was defined as the difference between the angle at the end of stance and minimum joint angle and the difference between the angle at footfall and minimum joint angle, respectively. These definitions presume that the limb (not including the hip point) is most flexed at footfall and most extended at the end of stance. Pelvic rotation was determined to be the dorsal (*x*–*z* plane), two-dimensional angle formed by a line connecting the hip and pelvis points, and a second line connecting the pelvis and eye points. Partial correlations of pelvic rotation with sprint speed and mass yielded no statistically significant effects (sprint speed, P=0.316; mass, P=0.714). As a result, the primary focus of variables presented here is on other limb joints and segments such as the knee, ankle, femur, tibia and foot. Three of the angles were measured relative to the water surface (i.e. the horizontal plane): foot–water (θ_{fw}), tibia–water (θ_{tw}) and body–water angles (θ_{bw}). Since θ_{bw} varied little through a stride, only the mean value was calculated. For θ_{fw} and θ_{tw}, calculated values included the angles at footfall, as well as the mean during stroke, and minimum and maximum angles during recovery.

Statistics

All digitized data were fit with a mean square error quintic spline algorithm following the method previously discussed by Walker (1998). Spline tolerance was determined to be the magnitude of data mean square error. Both linear and angular velocities were then calculated by taking the derivative of the resulting spline equation (from positional and angular data, respectively). All angular data were also calculated from the spline of positional data.

To examine the effects of size on kinematics, linear variables were adjusted by *SVL* and *LL*. Some previous studies on terrestrial lizard kinematics have scaled linear variables to lizard *SVL* (Irschick and Jayne, 2000; White and Anderson, 1994). It has been established that distal limb elements in lizards can scale negatively to lizard size (Garland, 1985; Irschick and Jayne, 2000; Marsh, 1988; White and Anderson, 1994). If linear bipedal locomotion parameters depend on hind limb motion, linear variables scaled by *SVL* downplay the actual variation with size. In the present study, all linear variables were normalized by *LL* (to more accurately reflect how animal size affects locomotor parameters) and by *SVL* (to permit comparisons with most established terrestrial lizard kinematic data). I performed simple linear regressions (StatView v.5.0.1) on these adjusted variables, with mass or

sprint velocity as the independent variable. Mass regressions were performed with all variables $\log_{10}$-transformed. Two-tailed *t*-tests were used to determine if regression slopes (α) were significantly different from that expected for isometric scaling.

Covariation between size and sprint velocity was statistically controlled by partial correlation analysis. Partial correlation permits determination of the relationship between an independent and dependent variable by holding the covariates constant. In the present study, partial correlations of velocity (holding mass constant) and mass (holding velocity constant) were completed in two ways. Correlation coefficients between absolute velocity and unadjusted dependent variables were determined by linear correlation. Correlation coefficients between mass and unadjusted dependent variables were determined by fitting a two-parameter, exponential equation to the data with a Gauss–Newton least squares estimation model. Partial correlation analyses were performed using Systat 9.0 (SPSS, Inc., Chicago, IL, USA).

Unless otherwise indicated, all data are presented as means ± S.E.M.

Results

Morphology

Assuming geometric scaling, limb segment lengths should scale logarithmically with mass and *SVL* with slopes of 0.33 and 1, respectively (Alexander, 1977; Alexander and Jayes, 1983; McMahon, 1975; Wainwright and Richard, 1995). Both tibia and femur lengths scaled isometrically with *SVL* (tibia, α=1.029±0.024; femur, α=0.964±0.027; Table 1), but only the tibia length scaled isometrically with mass; femur length scaled negatively with mass (Table 2). Foot length exhibited negative allometry with respect to both mass (α=0.277±0.006) and *SVL* (α=0.878±0.015). The basilisk lizard foot is extremely long, composing, on average, 44.2±0.2% of the total hindlimb length. The femur and tibia are much shorter and are approximately the same lengths (28.3±0.13% and 27.5±0.13%, respectively). As a result, total limb length (as measured by the sum of tibia, femur and foot lengths) was also negatively allometric. In other words, as the animal grew in length and mass, the relative length of the foot, and therefore total relative hindlimb length, decreased. *SVL* scaled negatively with mass, meaning that as the animal increased in mass, its body became proportionately shorter or stouter.

Table 1. *Scaling relationships of morphological variables with snout–vent length (SVL)*

Dependent variable	Slope	*y* intercept	r^2
Femur length (cm)*	0.964±0.027	–0.459±0.051	0.95
Tibia length (cm)*	1.029±0.024	–0.597±0.045	0.96
Foot length (cm)	0.878±0.015	–0.103±0.029	0.98
Total leg length (cm)	0.948±0.017	0.117±0.032	0.98

All variables $\log_{10}$-transformed.
P<0.0001 for the slopes of all regressions.
*Indicates isometric growth. All others are negatively allometric.
Values are means ± S.E.M. (N=72).

Table 2. *Scaling relationships of morphological variables with mass*

Dependent variable	Slope	*y* intercept	r^2
Snout–vent length (cm)	0.316±0.005	1.531±0.006	0.99
Femur length (cm)	0.304±0.009	1.018±0.012	0.94
Tibia length (cm)*	0.325±0.008	0.980±0.010	0.96
Foot length (cm)	0.277±0.006	1.243±0.008	0.97
Total leg length (cm)	0.298±0.006	1.572±0.008	0.97

All variables $\log_{10}$-transformed.
P<0.0001 for the slopes of all regressions.
*Indicates isometric scaling. All others are negatively allometric.
Values are means ± S.E.M. (N=72).

General stride kinematics

In all but three of the analyzed runs, the footfall pattern could be generalized as shown in Fig. 2. At any moment, there was always at least one foot in the water, and often both feet were in the water through all of slap and part of stroke. The three exceptional runs exhibited a short period (4–12 ms; 4–10% of a stride) during which there was an ‘aerial phase’ after stroke (i.e. both feet were simultaneously out of the water). This footfall pattern was exhibited only by basilisks weighing 8.9 g or less. Otherwise, footfall patterns changed little with increased mass (see Scaling section).

Fig. 3 shows the trajectories of the pelvis, hip, knee, ankle and MP (foot) points for a 20.8 g basilisk lizard, broken down into their three axial components. During the slap (13.9±5.2% of the stride; mean ± S.D.; N=15), basilisks spread the toes of the left foot and plunge it down laterally and backwards. During this phase, the pelvic girdle and trunk roll towards the left. In most recorded runs, the right foot is part way through recovery up but still submerged in water. The left arm swings in phase with the left foot at this time, moving downwards and backwards. The right arm always moves out of phase with the left arm.

With the toes still spread, basilisks then plantarflex and stroke through the water, pushing their left foot backwards and slightly down, finishing this phase with the foot sweeping medially to the body midline. The stroke phase makes up 17.5±5.1% (mean ± S.D.; N=15) of a stride. Midway through the stroke phase for the left foot, the right foot is extracted from the water and completes the recovery up phase. The left arm is held mostly steady, with the wrist approximately in line with the shoulder, or it begins a slow forwards and upwards sweep at this time.

The left foot now moves into the recovery up phase – the longest phase (49.1±4.4%; mean ± S.D.; N=15) of the stride – at the start of which basilisks adduct their toes and plantarflex the ankle such that the foot is approximately in line with the long axis of the tibia. Whereas the foot moves slightly caudad

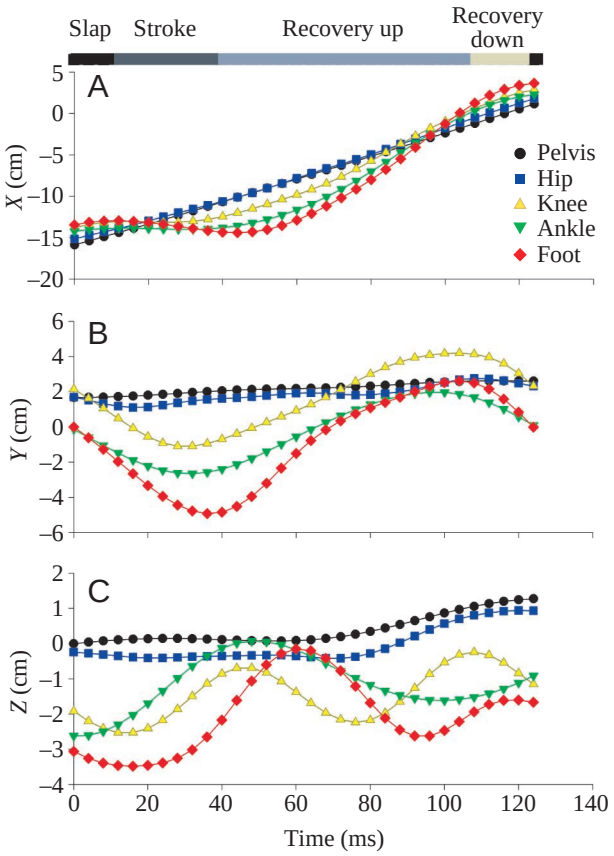

Fig. 3. A time series of pelvis and left hind limb point excursions in (A) *X*-, (B) *Y*- and (C) *Z*-axes over one stride for a 20.8 g lizard running at 1.2 m s^{-1}. The foot (MP) point experiences the greatest excursion along all three axes. The left foot footfall pattern is shown above A.

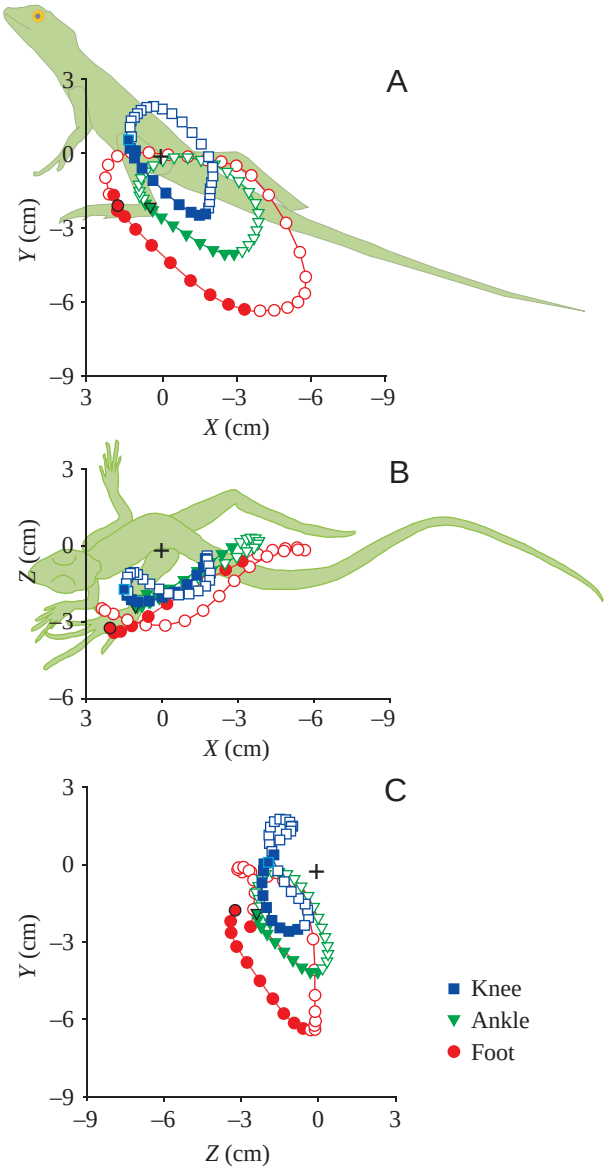

Fig. 4. (A) Lateral (*X*–*Y*), (B) dorsal (*X*–*Z*) and (C) posterior (*Z*–*Y*) views of limb points relative to the hip. Hip position is designated by a cross. Lizard images behind graphs show position of points relative to the lizard at the start of slap. The path of each point is counterclockwise in all three plots, starting with the points outlined in black (foot and ankle) or blue (knee). Solid points indicate stance phase, open points indicate swing (i.e. recovery) phase.

at the start of this phase, the primary motion of the foot is up, forwards and lateral. The pelvic girdle and trunk rock towards the right as the left foot is drawn out of the water in line with the axis of the hindlimb. After exiting the water, the ankle dorsiflexes such that the foot is toe up by the end of recovery up. The final part of recovery up is characterized by a near horizontal and forward movement of the foot, which brings it almost directly above where the next step begins. Basilisks then begin to abduct their toes in preparation for the next slap phase. About midway through this phase, the right foot begins its next step, completing most of slap and stroke as the left foot completes recovery up. The arm and leg movements on the left side are now approximately 90–170° out of phase, with the discrepancy of arm and leg movements in larger lizards exhibiting a greater phase shift.

The recovery down phase is short (19.5±6.8%; mean ± S.D.; *N*=15) and mostly involves the left foot moving down and medial to begin the next slap phase. The pelvic girdle once again begins to roll towards the left. At this time, the left arm is almost exactly out of phase with the leg: as the leg moves slightly forwards and down, the arm moves backwards and up. This phase completes the stride for the left foot as it contacts the water again, starting the slap phase for the next stride.

Basilisks' gait in dorsal view exhibited lateral undulations typical of reptilian locomotion. The eye and pectoral points moved out of phase with the midbody and pelvis points. The stride begins with the posterior half of the body concave left when the left foot first contacts the water. It becomes concave right by the end of the stroke, and bends back to concave left by the end of recovery up. The anterior half of the body follows a pattern opposite the posterior half of the body. The movement

of the midline points characterizes a slow traveling wave. Apart from one trial, the eye point consistently exhibited the greatest medio-lateral excursion during a stride, with the amplitude of lateral excursion decreasing posteriorly.

Throughout the stride, waves pass down the length of the tail, which is fully submerged underwater. Digitizing the maxima of these waves showed that the mean backwards velocity of the tail wave was 10.4±2.0% greater than the forward body velocity (one-tailed *t*-test, P=0.0014).

Limb linear and timing variables

Positions of each of the limb points are shown relative to a stationary hip point to better visualize the paths traced by the hindlimb through one stride (Fig. 4). The kinematics used on water are asymmetric, with the position of the hip located anterior to the centers of all three circular paths traced by the knee, ankle and foot. Furthermore, vertical excursion of the foot is much greater at the end of stance (filled points) than at slap (points outlined in black). In the dorsal aspect (*x*–*z* plane), medio-lateral excursions of limb points are large, moving as far as the body midline at maximum medial excursion. Finally, in the posterior view (*y*–*z* plane), the knee and foot points trace circular paths positioned primarily lateral to the hip. The knee traces a figure of eight, passing medial to lateral to medial from slap through recovery up and moving laterally during recovery down.

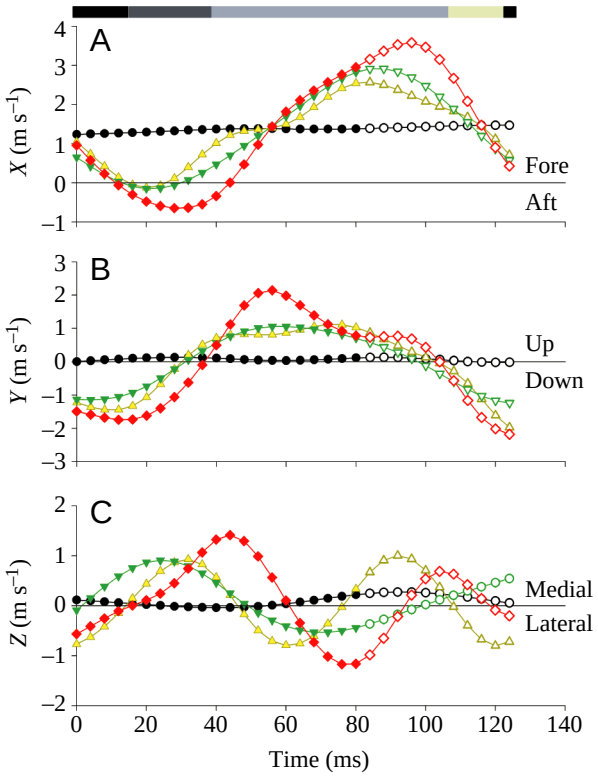

Fig. 5. Three time series of velocities of pelvis and left limb points in the three axes, for the same run as that presented in Fig. 3 (20.8 g, 1.4 m s^{-1}). The left foot footfall pattern is presented above A (see Fig. 3 for phase breakdown). Symbol definitions are as in Fig. 3. (A) Point velocities in the *X* (fore–aft) direction. All positive values indicate movement in the direction of motion, and all negative values indicate movement opposite the direction of motion. (B) Point velocities in the *Y* (vertical) direction. All positive values indicate movement upwards, and all negative values indicate movement downwards. (C) Point velocities in the *Z* (medio-lateral) direction. Positive values indicate medial movements, and negative values indicate lateral movements. Open symbols indicate when the foot is out of water, whereas closed symbols indicate that the foot is submerged.

Fig. 5 shows pelvis and hind limb point velocities over a stride. Foot velocities in the fore–aft direction had minima and maxima at the end of stroke and recovery up, respectively. Along the vertical axis, the foot moved most rapidly during slap (downwards) and during the first third of recovery up (upwards), when the foot was still in the water. After the foot exited the water, velocity plateaued until recovery down. Medio-lateral velocity fluctuations were large, with a slight phase delay distally along the hind limb.

All basilisks, regardless of size, ran at approximately the same absolute velocity (1.3±0.1 m s^{-1}), although the smallest lizard ran slower than the rest. Partial correlations for absolute velocity with mass held constant exhibited few significant correlations with kinematics (Table 3). Increased velocity coincided with a longer step length (r^2=0.65, P=0.005). Stride frequency did not vary with velocity (P=0.985). Other variables associated with increased velocity included increased knee and ankle horizontal excursions (ΔX_{knee}: r^2=0.64, P=0.005; ΔX_{ankle}: r^2=0.66, P=0.004), increased medio-lateral ankle excursion (r^2=0.41, P=0.045) and increased medio-lateral stroke speed (r^2=0.58, P=0.011). Ankle extension during stance decreased with increased velocity (r^2=0.45, P=0.033). Duration of each of the four stride phases – expressed as percentage of stride duration – did not have any correlation with sprint speed.

Despite the lack of variation in absolute running speeds over a size range, when all linear variables were adjusted for *LL* and *SVL*, many variables were found to be speed-dependent (Table 3). Higher relative velocities coincided with higher hip position at footfall ($Y_{hip,ff}$; P=0.002). Vertical hip excursion ($\Delta Y_{hip,stance}$) during stance did not vary with velocity. Basilisks increased relative sprint velocity ($\mathbf{U}_{avg}$) by increasing relative horizontal knee (ΔX_{knee}) and ankle excursions (ΔX_{ankle}) and thereby increasing relative stride length. They also decreased stride duration by shortening stance duration (Df_{stance}). Finally, they produced more thrust by increasing vertical foot stroke velocity ($\mathbf{U}_{Y,stroke}$), as well as medio-lateral foot velocity during both the slap ($\mathbf{U}_{Z,slap}$) and stroke phases ($\mathbf{U}_{Z,stroke}$).

Angular kinematics

Despite the large amount of variability in joint angles during a run, some patterns were observed between runs (Fig. 6). In all but the three lightest animals, ankle and knee angles at slap were less than 90°, indicating that the limb was highly flexed upon contact with the water. During slap, the ankle and knee only extended. Knee angle reached a maximum during the stroke phase (125±5°) and the ankle reached maximum

Table 3. *The effects of adjusted sprint speed on timing, angular and adjusted linear kinematic variables, with results from simple linear regressions and partial correlation analyses*†

Dependent variable	Slope	*y* intercept	r^2	*P*
Stride duration	–0.003±0.001	0.171±0.018	0.40 (0.44)	0.036 (0.026)
Df_{stance}	–0.007±0.002	0.402±0.031	0.53 (0.61)	0.011 (0.005)
Relative stride length**	0.092±0.019	0.574±0.290	0.71 (0.73)	0.001 (<0.001)
Relative ΔX_{knee}**	0.086±0.018	0.620±0.265	0.72 (0.74)	<0.001
Relative ΔY_{knee}	–	–	–	Ns
Relative ΔZ_{knee}	–	–	–	Ns
Relative ΔX_{ankle}**	0.089±0.019	0.582±0.281	0.71 (0.73)	0.001
Relative ΔY_{ankle}	–	–	–	Ns
Relative ΔZ_{ankle}*	0.018±0.004	0.066±0.056	0.72 (0.74)	<0.001
Relative $Y_{hip,ff}$	0.022±0.005	–0.119±0.075	0.68 (0.71)	0.002 (0.001)
Relative eLL_{slap}	0.013±0.004	0.215±0.067	0.49 (0.56)	0.017 (0.008)
Relative eLL_{stroke}	–	–	–	Ns
Knee extension	–4.45±0.74	136±11	0.80	<0.001
Knee flexion	–	–	–	Ns
Ankle extension*	–4.84±1.65	133±25	0.49 (0.43)	0.017 (0.029)
Ankle flexion	–	–	–	Ns
Relative $\mathbf{U}_{X,slap}$	–	–	–	Ns
Relative $\mathbf{U}_{X,stroke}$	–	–	–	Ns
Relative $\mathbf{U}_{Y,slap}$	–	–	–	Ns
Relative $\mathbf{U}_{Y,stroke}$	0.003±0.001	–0.110±0.016	0.46	0.022 (0.021)
Relative $\mathbf{U}_{Z,slap}$*	0.009±0.003	–0.107±0.045	0.52 (0.43)	0.013 (0.029)
Relative $\mathbf{U}_{Z,stroke}$	0.008±0.003	–0.020±0.039	0.48 (0.44)	0.018 (0.026)

†Only the absolute values were used in partial correlation analyses. Mass was held constant.

Asterisks indicate significant partial correlation of *absolute, unadjusted* dependent variable with absolute sprint velocity (mass held constant): *P<0.05; **P<0.01; ***P<0.001.

All linear variables used in simple linear regressions were adjusted by leg length (*LL*) and snout–vent length (*SVL*). When different, simple regression r^2 and/or *P*-values for *SVL* are shown in parentheses. All values not in parentheses are presented as means ± S.E.M. (N=11).

Abbreviations are presented as they are described in the text and List of symbols.

extension shortly thereafter at the beginning of recovery up (140±3°). Whereas adult basilisks flexed their knee more than juveniles at footfall (r^2=0.70, P=0.003), ankle angle at footfall exhibited no such pattern (r^2=0.32, P=0.088). There were also no significant correlations between mass and knee or ankle angles at the end of stance. It is particularly notable that the limbs exhibited only extension during a stride. Maximum hip extension angles were during slap and stroke (144±6° and 145±3°, respectively), and minimum extension angles usually occurred at the end of recovery up (116±2°). The hip was never flexed (i.e. <90°) throughout a stride, probably as a result of pelvic roll.

Dorsal and lateral video images showed that toes were widely abducted (i.e. spread) during slap and stroke and then adducted during recovery up. The toe adduction, in combination with near complete ankle extension during recovery up (165±2°), may have acted to streamline the foot and decrease the drag acting upon it during a period when it

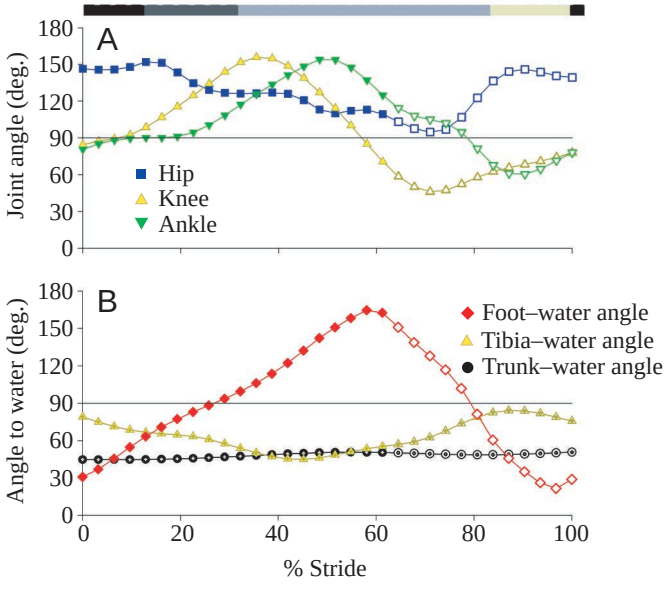

Fig. 6. Time series of three-dimensional angular excursions of (A) limb joints and (B) body segments relative to the water surface for the identical run presented in Figs 3–5. The left footfall pattern is indicated above A. All joint angles (A) greater than 90° indicate joint extension, whereas all angles less than 90° indicate flexion. Open symbols indicate when the foot is out of the water, whereas closed symbols indicate that the foot is submerged.

may not be producing any thrust. Upon exiting the water, the toes gradually abducted once more and were fully abducted by the end of recovery down.

Although body angle appeared to remain constant during a stride, the lightest and heaviest animals ran with more erect postures than did the medium basilisks (<10 g, 51±2°; 10–30 g, 46±1°; 60–80 g, 62±3°).

Scaling

Only two of the stride phases were size-dependent (Table 4) – the stroke phase increased and recovery down decreased in duration. Mean durations of each phase, as a percentage of the stride cycle, are presented in Fig. 2. Stride duration exhibited positive trends (P=0.055), indicating that heavier animals took fewer strides in a set period, with a greater proportion of the stride dedicated to the slap and stroke phases (Df_{stance}; P=0.004) or the total proportion of stride spent submerged in water (Df_{sub}; P=0.004).

Most angular variables scaled negatively with mass. As a lizard increased in mass, the limb was more flexed at slap, as indicated by decreased knee angle at footfall ($\theta_{knee,ff}$; P=0.003). Larger lizards also sank deeper into the water ($Y_{hip,min}$: r^2=0.61, P=0.007). There was clear size dependence with position of the foot to the water during slap (Fig. 7). Animals weighing ≤11.4 g slapped the water toe first or flat-footed (3±3°). There appeared to be a transition in foot position at around 20 g, as lizards around this mass slapped either flat-footed or heel first (–0.4±5°), and all but one of the heavier animals slapped the water heel first (–30±20°). One large adult (76.4 g) slapped the water toe first. However, in this case, the basilisk's hands touched the water; in the remaining analyzed runs, the hands were fully out of the water.

Adjusted linear variables describing limb excursion also reflected the more flexed limbs in adult basilisks (Table 4). Relative horizontal knee [$\Delta X_{knee(SVL)}$: r^2=0.47, P=0.029] and ankle [$\Delta X_{ankle(SVL)}$: r^2=0.44, P=0.037] values normalized by

Table 4. *Select results from partial correlation analysis and simple linear regressions† correlating absolute dependent variables (*dep. var.*) with basilisk mass as the independent variable*

Dependent variables	p_1	p_2	r^2_{mass}	p_3	p_4	$r^2_{velocity}$	$r^2_{mass\times velocity}$	P
ΔX_{knee} (cm)†	12.46	0.09	0.197	13.30	0.79	0.505	0.344	0.075
ΔY_{knee} (cm)*	2.09	0.27	0.842	4.96	–0.02	0.000	0.844	<0.001
ΔZ_{knee} (cm)*	0.90	0.35	0.799	3.07	–0.42	0.073	0.887	<0.001
ΔX_{ankle} (cm)†	12.53	0.09	0.186	13.20	0.84	0.525	0.336	0.081
ΔY_{ankle} (cm)*	2.13	0.29	0.955	5.39	–0.09	0.005	0.968	<0.001
ΔZ_{ankle} (cm)*	2.31	0.08	0.133	2.45	0.62	0.333	0.173	<0.001
$Y_{hip,ff}$ (cm)	3.06	–0.24	0.227	0.87	1.88	0.281	0.349	0.072
$Y_{hip,min}$ (cm)*	3.37	–0.40	0.431	0.43	2.82	0.249	0.615	0.007
eLL_{slap} (cm)†	2.45	0.13	0.370	3.43	0.22	0.047	0.377	0.059
eLL_{stroke} (cm)*	2.00	0.32	0.922	5.70	–0.12	0.007	0.938	<0.001
Stride length (cm)†	12.96	0.09	0.168	13.39	0.84	0.542	0.311	0.094
Stride duration (s)†	0.10	0.10	0.383	0.13	–0.04	0.003	0.388	0.055
Df_{stance}*,†	0.22	0.11	0.500	0.34	–0.31	0.203	0.665	0.004
Df_{sub}*,†	0.47	0.09	0.612	0.65	–0.18	0.107	0.713	0.004
$\mathbf{U}_{X,slap}$ (m s^{-1})	0.20	0.04	0.002	0.22	0.03	0.000	0.002	0.900
$\mathbf{U}_{X,stroke}$ (m s^{-1})*,†	–0.02	0.74	0.424	–0.34	–1.01	0.068	0.472	0.028
$\mathbf{U}_{Y,slap}$ (m s^{-1})*,†	–0.65	0.26	0.548	–1.53	–0.19	0.016	0.567	0.012
$\mathbf{U}_{Y,stroke}$(m s^{-1})*,†	–0.16	0.45	0.767	–0.77	–0.60	0.091	0.872	<0.001
Knee extension (deg.)*,†	34.21	0.24	0.567	83.69	–0.54	0.179	0.727	0.001
Ankle extension (deg.)	30.17	0.24	0.184	85.83	–1.19	0.381	0.337	0.078
$\theta_{knee,ff}$ (deg.)*,†	137.37	–0.20	0.691	75.72	0.08	0.004	0.700	0.003
$\theta_{knee,es}$ (deg.)†	173.61	–0.06	0.311	144.88	–0.02	0.002	0.310	0.094
$\theta_{ankle,ff}$ (deg.)	109.59	–0.12	0.261	67.53	0.47	0.129	0.319	0.088
$\theta_{ankle,es}$ (deg.)	140.23	–0.01	0.005	145.91	–0.30	0.14	0.003	0.869
% Slap	0.12	0.03	0.015	0.12	0.32	0.079	0.013	0.750
% Stroke*,†	0.11	0.18	0.320	0.22	–0.66	0.277	0.481	0.026
% Recovery up	0.48	0.01	0.024	0.50	0.02	0.004	0.23	0.672
% Recovery down*,†	0.33	–0.19	0.389	0.16	0.60	0.122	0.466	0.030

Variables were fitted to the following two nonlinear, exponential functions: *dep. var.* = $p_1 \times (mass^{p_2})$ and *dep. var.* = $p_3 \times (velocity^{p_4})$. Unknown parameters ($p_1$, p_2, p_3 and p_4) were determined by Gauss–Newton estimations.

Abbreviations are presented as described in the text and List of symbols: ff, footfall; es, end of stance.

P-values were determined with two-tailed t-tests: *indicates significance of P<0.05.

†Indicates a significant simple linear regression of dependent variable against mass. All linear variables were adjusted by snout–vent length (*SVL*) and leg length (*LL*) (P<0.05)

N=11, except Df_{sub}, which was N=10.

SVL decreased with increasing size. No size-dependent trend was observed for relative vertical joint excursions of the knee and ankle, although their absolute vertical excursions were closely associated with mass (ΔY_{knee}: r^2=0.84, P<0.001; ΔY_{ankle}: r^2=0.97, P<0.001). Finally, relative medio-lateral excursions exhibited significant negative allometry only at the ankle [$\Delta Z_{ankle(SVL)}$: r^2=0.44, P=0.035]. Other normalized linear variables that were negatively allometric to lizard mass included $Y_{hip,ff(SVL)}$ (r^2=0.76, P=0.002), $eLL_{slap(SVL)}$ (r^2=0.51, P=0.021), stride length$_{(SVL)}$ (r^2=0.44, P=0.036) and relative $\mathbf{U}_{avg(SVL)}$ (r^2=0.70, P=0.003). Linear variables normalized by *LL* exhibited fewer significant trends because the lightest basilisk (2.8 g) exhibited unusually low, outlying values – probably a result of its disproportionately long legs; however, when values from the lightest basilisk are removed, scaling by *SVL* and *LL* exhibit the same trends. In most cases, variables scaled by *LL* have greater correlations with mass than do linear variables scaled by *SVL*.

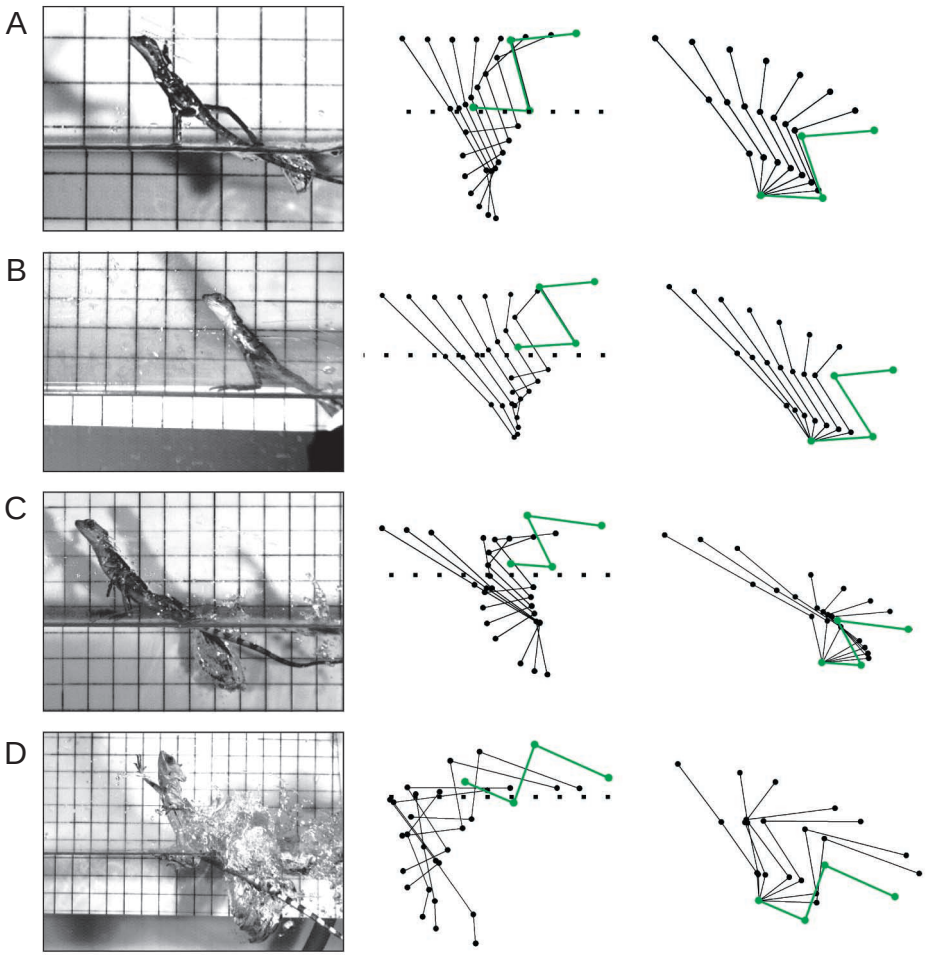

Fig. 7. Limb positions relative to size for juvenile to adult basilisks. The left-hand column shows a series of frames of a basilisk at the start of slap for a size range of lizards. The backgrounds of the frames are all 2 cm×2 cm grids. The central and right-hand columns are two-dimensional overlaid stick figures of limb positions during the support phase of aquatic running for the run represented in the adjacent frame. The hip, knee, ankle and foot (i.e. metatarsal–phalangeal) points are represented in each set of figures, with the hip at the upper end and the foot at the lower end of each stick figure. In all three columns, the basilisk is running from the right to the left. The dotted, horizontal line in the central column represents water level. The right-hand column figure is created from the same trial as the figure in the left-hand column, but with the position of the toe fixed. The highlighted (green) stick figure represents the limb position shown in the left-hand column video frame. Relative velocities were calculated by dividing by snout–vent length (*SVL*) and are presented as body lengths per second (L s^{-1}). (A) 2.8 g, 0.84 m s^{-1} or 17.8 L s^{-1}; (B) 11.4 g, 1.6 m s^{-1} or 21.2 L s^{-1}; (C) 20.8 g, 1.38 m s^{-1} or 15.2 L s^{-1}; (D) 78.0 g, 1.00 m s^{-1} or 7.56 L s^{-1}. At comparable speeds (A–C), heavier lizards exhibited greater limb excursions. Also, whereas lighter lizards (weighing <20 g; A,B) usually slapped the water surface toe first or flat-footed, heavier lizards (>20 g; C,D) slapped the water heel first.

Discussion

Basilisks ran across water surprisingly slowly in comparison with other lizards of similar morphology (e.g. the zebra-tailed lizard *Callisaurus draconoides* and the Mojave fringe-toed lizard *Uma scoparia*). *C. draconoides* and *U. scoparia* maximum sprint velocities on land are over 4 m s^{-1} (Irschick and Jayne, 1999), whereas basilisks in the present study ran at maximum speeds of about 1.6 m s^{-1} on water. At slow running speeds, desert iguanas (*Dipsosaurus dorsalis*) of various sizes exhibited many size-dependent kinematic differences due largely to juvenile iguanas' proportionately longer legs (Irschick and Jayne, 2000). Basilisk water-running kinematics support these results since most kinematic variation observed in this study resulted from differences in size rather than running speed.

Basilisk kinematics and kinetics

The kinematics of basilisk water running varied considerably. Basilisks weighing up to 20 g sometimes exhibited an aerial phase in a run. Yet it was unclear which variables other than mass were responsible for this variability. In general, the forearms 'windmill' during a run but to different extents. When basilisks ran with a large trunk angle to the water, they extended their arms forwards with minimal rotation around the shoulder. By contrast, when the trunk was held at ~45° to the water – the much more common body posture – basilisks' arm movements matched directions with the leg on the contralateral side. In

other runs, the arms moved with a slight delay to the contralateral hindlimb and were sometimes so delayed that it nearly matched the movements with the hindlimb on the same side. Windmilling the forearms may serve to counteract torques placed on the body during a stride, as have been reported in human studies to explain the pendulum-like motion of the arms during walking (Li et al., 2001).

The function of the tail in lizard locomotion has been largely ignored in most previous studies; yet the tail may play a major role as a counterbalance in basilisk lizard locomotion (Snyder, 1949, 1962) since it makes up ~18% of basilisks' total body mass (present study). Basilisks drag their tails behind them while running through water (Fig. 1). The mass of the fluid above the tail and skin frictional drag from the fluid surrounding the tail could thus aid in keeping basilisks in an upright posture.

The tail may also produce some thrust as basilisks run. The wave velocity traveling posteriorly along the tail exceeds the forward velocity of the body on average by 10.4%. This classically would indicate that the tail is generating some thrust. In larger basilisks, the tail is laterally compressed at the base, which would aid in thrust generation. However, since the rest of the exceptionally long tail tapers to a very fine point, it is unclear whether it could generate enough thrust to add substantially to the forward progression of the animals.

Problems associated with sinking into a surface add another level of complexity to basilisks' locomotion. Basilisks reduce hydrodynamic drag on the foot in two ways: by avoiding submersion of the foot in water (Snyder, 1949) and by adducting the toes during recovery up (Glasheen and McMahon, 1996a; present study). When basilisks slap the water, they create an air-filled cavity surrounding their foot. Using a model of a basilisk foot, approximated as a circular disk, Glasheen and McMahon (1996a,b) predicted that basilisks need to run at a minimum stride frequency ($f_{str,min}$) that would allow them to retract their foot out of the water prior to the time of air cavity closure (t_{seal}) and thus minimize hydrodynamic drag on the foot. Results from the present study support this prediction since all measured lizard stride frequencies were greater than the predicted $f_{str,min}$.

Since the value of $f_{str,min}$ is based upon a measured t_{seal}, cavity geometry substantially influences the predicted value for $f_{str,min}$. The foot missile (Glasheen and McMahon, 1996a,b) was dropped vertically and therefore does not simulate the lizards' stride with kinematic accuracy. In an actual run, the final water cavity is formed during the stroke phase of the stride. If the shape of the cavity created during the slap phase – or during the vertical disk drop – is approximated as a cylinder with its long axis positioned vertically, the cavity created during the stroke is a cylinder on its side. The area of the cavity at water level would thus be much greater in the cavity created during stroke than that created during slap. Investigations on the behavior of air bubbles in fluids have shown that the lowest energy shape for a bubble is a sphere. As a result, the cylindrical cavities created in each phase would collapse towards a spherical shape. How this would affect t_{seal} remains to be examined.

Although kinematic analysis provides only a preliminary insight into the production of motion, it does permit some qualitative predictions about the mechanics of motion. All basilisks weighing <20 g slapped the water slightly toe first or flat-footed, indicating that the majority of force generated was initially lift rather than thrust. Basilisks heavier than 30 g slapped the water heel first. As a result of the foot orientation, this suggests that the large basilisks should experience reductions in forward velocity during slap due to the production of thrust counter to the direction of motion. The basilisks' ability to run through water is highly influenced by its running speed (Rand and Marx, 1967), and the slap impulse produced is dependent on foot size to the third power (Glasheen and McMahon, 1996a,b). It is therefore interesting to note that, irrespective of size, all basilisks ran at similar absolute velocities – as has been reported in field studies (Rand and Marx, 1967).

Additional insight into the novel kinematics of aquatic running may be gained from human swimming. Basilisk limb movements during the stroke phase of water running are surprisingly similar to the arm kinematics recorded for competitive swimmers during the propulsive stroke of front-crawl (i.e. 'freestyle') swimming. The shoulder of a swimmer is analogous to the pelvic girdle of a basilisk, and a swimmer's arms are analogous to a basilisk's hindlimbs. During the propulsive stroke, the arm moves down, back and medially, as does a basilisk hindlimb. Although the actual function of the medial sweep remains controversial, hypotheses on how it increases propulsive forces in swimming have included (1) the curved hand path increasing the distance traversed by the hand, and thereby allowing a greater amount of propulsive force to be produced over a stroke, and (2) the medial movement allowing larger muscle groups to be utilized for propulsion. A contrasting view is that the medial movement results from the natural body roll associated with this style of swimming and thus does not necessarily enhance swimming performance (Hay et al., 1993; Liu et al., 1993). The relevance of these limb movements to water running remains to be determined, although the aforementioned hypotheses do provide some initial ideas.

Effects of size on kinematic variables

Juveniles ran proportionately much faster than did adults because of their smaller size. In the present study, those animals that ran at a higher adjusted speed also maintained a significantly greater relative hip height at footfall. The ability to stay on water relies on a combination of forces generated during the slap and stroke (Glasheen and McMahon, 1996a,b) and was affected more by basilisk size than sprint speed. Forces produced by a slap impulse among juvenile lizards can make up more than 60% of the needed impulse to stay on water; yet, during the same phase, adult basilisks can produce only about 10–20% of the necessary force to stay on water (Glasheen and McMahon, 1996a,b). As a result, maximizing force production during the stroke phase – as opposed to during slap – becomes even more important to adult basilisks. This

can manifest itself as an extended stroke phase or faster stroke speed with increased basilisk mass.

Adult basilisks do employ an extended stance phase, as indicated by increased duty factor and prolonged stroke phase duration. However, they also stroke through the water with slower absolute velocities than do juveniles. Adults do not exhibit greater fore–aft ankle excursions over a stride, so the prospect of producing less force over a longer distance for ultimately greater total force production also seems unlikely. Finally, adult basilisks potentially produce less power at footfall than do juveniles. A study examining power output during two-legged jumps in humans reported maximum power output between knee angles of 110° and 130° (Zamparo et al., 1997). Although none of the mean basilisk knee angles at footfall are within the range of the power plateau for humans, the smallest basilisks weighing less than 10 g come closest to this range (104±6°). The largest lizards fall far outside this range (59±8°). If power curves generated by basilisks are similar to those generated by humans, then large basilisks are producing much less power with their hind limbs at slap.

The results show that large basilisks are simply at a disadvantage. Their disproportionately greater mass, smaller feet and slower relative running speed all contribute to increased difficulty running through water.

Aquatic versus terrestrial locomotion

When walking on a stiff surface, work done on the environment is close to zero, assuming the foot does not slip or move the substratum. Most of the work done by the muscles and tendons in the first half of a step is therefore absorbed and stored in the stretched elements as elastic energy (Cavagna, 1985; Farley and González, 1996; McMahon and Greene, 1979). This energy storage manifests itself as flexion of both the ankle and knee joints, as reported in terrestrial running humans (Farley and González, 1996; Ferris et al., 1998; Gatesy and Biewener, 1991; Lejeune et al., 1998; McMahon and Greene, 1979) and lizards (Fieler and Jayne, 1998; Irschick and Jayne, 1999, 2000; Jayne and Irschick, 1999). By contrast, when running on water, basilisks only extended their ankle and knee joints during stance (slap and stroke phases). This suggests that unlike during land runs, the muscles and tendons in basilisk legs no longer serve a dual function for producing force and for storing elastic energy; instead, they are used only to produce force.

Basilisk trunk angle decreased the most during the recovery phases in terrestrial (Snyder, 1949) and aquatic (present study) runs. However, basilisks run with a more upright posture during aquatic runs (52±2°) than they do during terrestrial runs (8–15°; Snyder, 1949), indicating that their center of mass is shifted caudally when running through water. Lateral undulations of the trunk are similar when running through water or on land but exhibit much more exaggerated amplitudes when running through water (Laerm, 1973). This may result from the foot sinking into the surface, forcing the body to undergo greater axial rotation during stance. Pelvic rotation was much greater in aquatic runs for basilisk lizards (87°–97°) than for terrestrial runs among other bipedal lizards (45°–55°; Irschick and Jayne, 1999).

Limb excursion during a stride across water is greater than that on land. During terrestrial basilisk runs, limb joint positions never exceed hip height and are kinematically symmetrical; the *eLL* (linear distance between H and MP points) at the beginning of stance is only slightly shorter (91%) than the *eLL* at the end of stance (Snyder, 1949, 1954). Similar results are also reported for other bipedal lizards (Irschick and Jayne, 1999), birds and humans (Gatesy and Biewener, 1991). On water, limb joints exceed or match hip height, and the *eLL* at the end of stroke is up to three times as long as the *eLL* at footfall (Fig. 4A). Since the greatest amount of propulsion is produced between the time the foot passes beyond the hip to the end of stance (Snyder, 1949), the greatest propulsive phase would last about 50% of the stance period in symmetric terrestrial runs. However, in aquatic running, as a result of greater limb retraction caudad, the propulsive phase lasts a proportionately greater duration for one stride. On a surface that is so much more yielding than solid ground, and also slips with each step (Laerm, 1973), an extended propulsive phase for more sustained force production (both lift and thrust) would be important to keep the lizard's center of mass at a constant height above water.

Strategies to increase sprint speed through water are similar to those used on land by other tetrapods. On water, relative sprint speed is increased by lengthening the stride and increasing stride frequency (Table 3). Stride length probably plays a larger role in increasing sprint speed than does stride frequency, as evidenced by its steeper regression slope. Quadrupedal lizards running on land (Fieler and Jayne, 1998), humans (Gatesy and Biewener, 1991) and birds (Gatesy and Biewener, 1991) have all shown similar trends. However, contrary to recent findings indicating lizards adopt a more extended limb posture at higher sprint speeds (Irschick and Jayne, 1998; Jayne and Irschick, 1999), basilisks assume a more crouched posture.

The present study has focused on water-running kinematics. Actual forces generated during water running are still unknown. Future work will include an analysis of the magnitude and direction of forces involved in basilisk aquatic running, using particle imaging velocimetry (PIV) to visualize fluid motion. This technique has already been applied numerous times to fish swimming studies for the analysis of fin function (e.g. Drucker and Lauder, 1999; Lauder, 2000; Liao and Lauder, 2000) and insect flight (Birch and Dickinson, 2001; Dickinson et al., 1999). Other directions will involve measuring kinematics and forces produced by basilisks running bipedally on land, so that a direct comparison can be made for how locomotor strategy changes in response to different surface properties.

List of symbols

ΔX	horizontal joint excursion
ΔY	vertical joint excursion
ΔY_{hip}	total vertical hip excursion

ΔZ	medio-lateral joint excursion
Df	duty factor
Df_{stance}	duty factor calculated for the fraction of a stride dominated by the slap and stroke phases
Df_{stance}	duty factor calculated for the fraction of a stride spent underwater
Df_{sub}	duty factor calculated for the fraction of a stride in which the foot is submerged in water
eLL	effective limb length
eLL_{ff}	effective limb length quantified at footfall
eLL_{stroke}	mean effective limb length for the stroke phase
$f_{str,min}$	minimum stride frequency
LL	leg length
SVL	snout–vent length
t_{seal}	time of air cavity closure
$\mathbf{U}_{avg}$	mean forward velocity
$\mathbf{U}_{Y,stroke}$	vertical foot stroke velocity
$\mathbf{U}_{Z,slap}$	medio-lateral foot slap velocity
$\mathbf{U}_{Z,stroke}$	medio-lateral foot stroke velocity
Y_{hip}	mean height of the hip relative to the water surface
$Y_{hip,max}$	maximum height of the hip in a stride
$Y_{hip,min}$	minimum height of the hip in a stride
θ_{ankle}	three-dimensional ankle angle
θ_{bw}	angle of body relative to the water surface
θ_{fw}	angle of foot relative to the water surface
θ_{hip}	three-dimensional hip angle
$\theta_{hip,es}$	angle of hip calculated at end of stance
$\theta_{hip,ff}$	angle of hip calculated from positional data at footfall
$\theta_{hip,min}$	minimum angle of hip at stance
θ_{knee}	three-dimensional knee angle
θ_{tw}	angle of tibia relative to the water surface

I thank Andrew Biewener, Jimmy Liao, Peter Madden, Jen Nauen, Howard Stone and Eric Tytell for the many helpful suggestions they volunteered throughout the length of this project. I am grateful to Jim Glasheen for leaving his old basilisk water-running track for my use and also for his guidance at the start of this study. I also thank Monica Daley, Ty Hedrick, Bruce Jayne, Russell Main, Craig McGowan and Jim Usherwood for providing valuable comments on the manuscript. I owe a special thanks to George Lauder for providing me with the equipment and academic and financial support, all of which were critical to make this project possible. This study was supported by National Science Foundation grant 9807021 to G.V.L. for general support, a graduate student research grant from the Department of Organismic and Evolutionary Biology at Harvard University to S.T.H. and a National Science Foundation Graduate Research Fellowship to S.T.H.

References

Alexander, R. McN. (1977). Mechanics and scaling of terrestrial locomotion. In *Scale Effects in Animal Locomotion* (ed. T. J. Pedley), pp. 93-110. London: Academic Press.

Alexander, R. McN. and Jayes, A. S. (1983). A dynamic similarity hypothesis for the gaits of quadrupedal mammals. *J. Zool.* **201**, 135-152.

Barden, A. (1943). Notes on the basilisk at Barro Colorado Island, Canal Zone. *Copeia* **24**, 407-408.

Bertram, J. E. A. and Biewener, A. A. (1992). Allometry and curvature in the long bones of quadrupedal mammals. *J. Zool.* **226**, 455-467.

Biewener, A. A. (1983). Allometry of quadrupedal locomotion: the scaling of duty factor, bone curvature and limb orientation to body size. *J. Exp. Biol.* **105**, 147-171.

Birch, J. M. and Dickinson, M. H. (2001). Spanwise flow and the attachment of the leading-edge vortex on insect wings. *Nature* **412**, 729-733.

Cavagna, G. A. (1985). Force platforms as ergometers. *J. Appl. Phys.* **39**, 174-179.

Cavagna, G. A., Heglund, N. C. and Taylor, C. R. (1977). Walking, running and galloping: mechanical similarities between different animals. In *Scale Effects in Animal Locomotion* (ed. T. J. Pedley), pp. 111-125. London: Academic Press.

Dickinson, M. H., Lehmann, F.-O. and Sane, S. P. (1999). Wing rotation and the aerodynamic basis of insect flight. *Science* **284**, 1954-1960.

Drucker, E. G. and Lauder, G. V. (1999). Locomotor forces on a swimming fish: three-dimensional vortex wake dynamics quantified using digital particle image velocimetry. *J. Exp. Biol.* **202**, 2393-2412.

Farley, C. T., Glasheen, J. W. and McMahon, T. A. (1993). Running springs: speed and animal size. *J. Exp. Biol.* **185**, 71-86.

Farley, C. T. and González, O. (1996). Leg stiffness and stride frequency in human running. *J. Biomech.* **29**, 181-186.

Ferris, D. P., Louie, M. and Farley, C. T. (1998). Running in the real world: adjusting leg stiffness for different surfaces. *Proc. R. Soc. Lond. Ser. B. Biol. Sci.* **265**, 989-994.

Fieler, C. L. and Jayne, B. C. (1998). Effects of speed on the hindlimb kinematics of the lizard *Dipsosaurus dorsalis*. *J. Exp. Biol.* **201**, 609-622.

Garland, T. J. (1985). Ontogenetic and individual variation in size, shape and speed in the Australian agamid lizard *Amphibolurus nuchalis*. *J. Zool.* **207**, 425-439.

Gatesy, S. M. and Biewener, A. A. (1991). Bipedal locomotion: effects of speed, size and limb posture in birds and humans. *J. Zool.* **224**, 127-147.

Glasheen, J. W. and McMahon, T. A. (1996a). A hydrodynamic model of locomotion in the basilisk lizard. *Nature* **380**, 340-342.

Glasheen, J. W. and McMahon, T. A. (1996b). Size-dependence of water-running ability in basilisk lizards (*Basiliscus basiliscus*). *J. Exp. Biol.* **199**, 2611-2618.

Hatze, H. (1988). High-precision three-dimensional photogrammetric calibration and object space reconstruction using a modified DLT-approach. *J. Biomech.* **21**, 533-538.

Hay, J. G., Liu, Q. and Andrews, J. G. (1993). The influence of body roll on handpath in freestyle swimming: a computer simulation study. *J. Appl. Biomech.* **9**, 227-237.

Hedrick, T. L., Tobalske, B. W. and Biewener, A. A. (2002). Estimates of circulation and gait change based on a three-dimensional kinematic analysis of flight in cockatiels (*Nymphicus hollandicus*) and ringed turtle-doves (*Streptopelia risoria*). *J. Exp. Biol.* **205**, 1389-1409.

Heglund, N. C., Taylor, C. R. and McMahon, T. A. (1974). Scaling stride frequency and gait to animal size: mice to horses. *Science* **186**, 1112-1113.

Huey, R. B. and Hertz, P. E. (1982). Effects of body size and slope on sprint speed of a lizard (*Stellio (Agama) Stellio*). *J. Exp. Biol.* **97**, 401-409.

Irschick, D. J. and Jayne, B. C. (1998). Effects of incline on speed, acceleration, body posture, and hindlimb kinematics in two species of lizard *Callisaurus draconoides* and *Uma scoparia*. *J. Exp. Biol.* **201**, 273-287.

Irschick, D. J. and Jayne, B. C. (1999). Comparative three-dimensional kinematics of the hindlimb for high-speed bipedal and quadrupedal locomotion of lizards. *J. Exp. Biol.* **202**, 1047-1065.

Irschick, D. J. and Jayne, B. C. (2000). Size matters: ontogenetic variation in the three-dimensional kinematics of steady-speed locomotion in the lizard *Dipsosaurus dorsalis*. *J. Exp. Biol.* **203**, 2133-2148.

Jayne, B. C. and Irschick, D. J. (1999). Effects of incline and speed on the three-dimensional hindlimb kinematics of a generalized iguanian lizard (*Dipsosaurus dorsalis*). *J. Exp. Biol.* **202**, 143-159.

Laerm, J. (1973). Aquatic bipedalism in the basilisk lizard: the analysis of an adaptive strategy. *Am. Midl. Nat.* **89**, 314-333.

Lauder, G. V. (2000). Function of the caudal fin during locomotion in fishes: Kinematics, flow visualization, and evolutionary patterns. *Am. Zool.* **40**, 101-122.

Lejeune, T. M., Willems, P. A. and Heglund, N. C. (1998). Mechanics and energetics of human locomotion on sand. *J. Exp. Biol.* **201**, 2071-2080.

Li, Y., Wang, W., Crompton, R. H. and Gunther, M. M. (2001). Free vertical moments and transverse forces in human walking and their role in relation to arm-swing. *J. Exp. Biol.* **204**, 47-58.

Liao, J. and Lauder, G. V. (2000). Function of the heterocercal tail in white sturgeon: flow visualization during steady swimming and vertical maneuvering. *J. Exp. Biol.* **203**, 3585-3594.

Liu, Q., Hay, J. G. and Andrews, J. G. (1993). The influence of body roll on handpath in freestyle swimming: an experimental study. *J. Appl. Biomech.* **9**, 238-253.

Marsh, R. L. (1988). Ontogenesis of contractile properties of skeletal muscle and sprint performance in the lizard *Dipsosaurus dorsalis*. *J. Exp. Biol.* **137**, 119-139.

Maturana, H. R. (1962). A study of the species of the genus *Basiliscus*. *Bull. Mus. Comp. Zool.* **128**, 1-34.

McMahon, T. A. (1975). Using body size to understand the structural design of animals: quadrupedal locomotion. *J. Appl. Phys.* **39**, 619-627.

McMahon, T. A. and Greene, P. R. (1979). The influence of track compliance on running. *J. Biomech.* **12**, 893-904.

Rand, A. S. and Marx, H. (1967). Running speed of the lizard *Basiliscus basiliscus* on water. *Copeia* **1967**, 230-233.

Reilly, S. M. and Delancey, M. J. (1997a). Sprawling locomotion in the lizard *Sceloporus clarkii*: quantitative kinematics of a walking trot. *J. Exp. Biol.* **200**, 753-765.

Reilly, S. M. and Delancey, M. J. (1997b). Sprawling locomotion in the lizard *Sceloporus clarkii:* the effects of speed on gait, hindlimb kinematics, an daxial bending during walking. *J. Zool.* **243**, 417-433.

Reinschmidt, C. and van den Bogert, T. (1997). *Kinemat: A MATLAB Toolbox For Three-Dimensional Kinematic Analyses*. Calgary: Human Performance Laboratory, The University of Calgary.

Russell, A. P. and Bels, V. L. (2001). Biomechanics and kinematics of limb-based locomotion in lizards: review, synthesis and prospectus. *Comp. Biochem. Physiol. A* **131**, 89-112.

Snyder, R. C. (1949). Bipedal locomotion of the lizard *Basiliscus basiliscus*. *Copeia* **1949**, 129-137.

Snyder, R. C. (1952). Quadrupedal and bipedal locomotion of lizards. *Copeia* **1952**, 64-70.

Snyder, R. C. (1954). The anatomy and function of the pelvic girdle and hindlimb in lizard locomotion. *Am. J. Anat.* **95**, 1-45.

Snyder, R. C. (1962). Adaptations for bipedal locomotion of lizards. *Am. Zool.* **2**, 191-203.

Wainwright, P. C. and Richard, B. A. (1995). Scaling the feeding mechanism of the largemouth bass (*Micropterus salmoides*): motor pattern. *J. Exp. Biol.* **198**, 1161-1171.

Walker, J. A. (1998). Estimating velocities and accelerations of animal locomotion: a simulation experiment comparing numerical differentiation algorithms. *J. Exp. Biol.* **201**, 981-995.

White, T. D. and Anderson, R. A. (1994). Locomotor patterns and costs as related to body size and form in teiid lizards. *J. Zool.* **233**, 109-128.

Woltring, H. J. and Huiskes, R. (1990). Stereophotogrammetry. In *Biomechanics of Human Movement* (ed. N. Berme and A. Capozzo), pp. 108-127. Worthington, OH: Bertec Corporation.

Zamparo, P., Antonutto, G., Capelli, C., Girardis, M., Sepulcri, L. and di Prampero, P. E. (1997). Effects of elastic recoil on maximal explosive power of the lower limbs. *Eur. J. Appl. Phys.* **75**, 289-297.